# Harmonic Generation in Multipactor Discharges

Patrick Y. Wong, *Member, IEEE*, Peng Zhang, *Senior Member, IEEE*, and John P. Verboncoeur, *Fellow, IEEE*

***Abstract*— Multipactor, a sustained electron avalanche driven by radiofrequency (RF), has been extensively studied due to its importance in all RF vacuum electronic devices. In particular, much effort has been made in understanding the phenomenon to mitigate it in real systems. On the other hand, some have used what is often seen as a disastrous effect for benefit. In this article, we study a novel way of using multipactor discharges for harmonic generation. We take advantage of the intrinsic phase-focusing mechanism of multipactor as a natural charge-bunching mechanism. The theory along with some validating test cases will be presented. Potential (beneficial) applications and ramifications of this phenomenon will be briefly discussed.**

***Index Terms*— Harmonics, multipactor.**

## I. Introduction

MULTIPACTOR is a resonant ac discharge of secondary electrons that can occur in any radiofrequency (RF) vacuum electronic system. More often than not, it is undesirable because of its adverse effects, which include, but are not limited to, detuning and $Q$-reduction of an RF cavity, localized heating, distortion of signals, and so on. [1]–[4]. However, there have been a few instances where this electron avalanche was beneficial. In particular, Mako and Peter [5] proposed using two-surface multipactor as an electron source for a pulsed electron gun. Given the right conditions, stray electrons born from any number of processes can become phase locked to an RF signal. These electrons will then bounce back and forth between the two plates and can generate secondary electrons from their impacts, leading to an avalanche. Consequently, the "beam" current of this electron cloud becomes amplified. If, as Mako and Peter [5] proposed, one of the electrodes was partially transparent (a "double-screen"), a portion of the multipactor electrons may escape to form the desired electron beam (similar to the internal workings of a laser cavity).

Because of the random nature of electron emission from a surface, one can imagine that electrons may be born from a surface with different initial velocities and at different times. Hence, there may be crossing of the electrons' orbits in the gap between the plates. From klystron and traveling-wave tube (TWT) theory [6]–[8], this charge overtaking (or in the less extreme case, orbital or current crowding) is the mechanism behind harmonic generation. In this article, we will explore the possibility of harmonic generation in the electron clouds in multipactor by utilizing a simple (1-D) planar model [9] (Fig. 1). We will demonstrate charge overtaking and/or current crowding and calculate the resulting harmonic currents. This may give some insights into the observed harmonics in the beam current as well as the radiation fields from the multipactor. The conditions of when this mechanism is valid (coherence) and how important the effects are will be assessed in this article along with potential applications and ramifications.

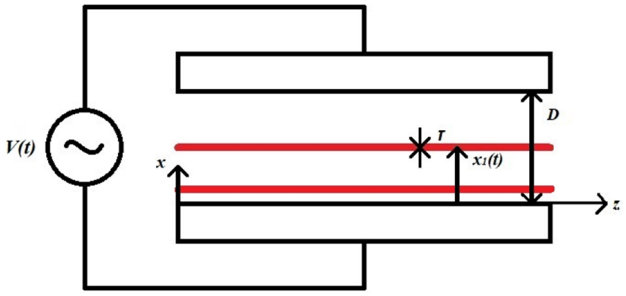


Fig. 1. Schematic of a 1-D 2-surface planar multipactor.

This article is different from what was done in the previous literature. In particular, Semenov *et al.* [10] considered the motion of a single macroparticle in a parallel-plate geometry subject only to the sinusoidal electric field. From here, the "beam" current was decomposed into an oscillatory part (at the driving frequency) and a "free" part that may be rewritten as a Fourier series consisting of harmonics of the driving signal. This, however, was applied on a *global* scale (i.e., at the output, with knowledge of all the transits of the multipactor electrons between the plates) to give a simple explanation of RF noise from the multipactor. Gimeno *et al.* [11] and Sorolla *et al.* [12] explained the radiation fields from a parallel-plate multipactor by expanding the charged particle current in a Fourier series. However, similar to Semenov *et al.* [10], they considered the expansion of the current (in the case of Sorolla *et al.* [12], the spatially averaged current; more on this has been discussed later) in a *global* manner. Here, however, we represent the current of the electron cloud (a collection of electrons) in a Fourier series (of infinite harmonics) *per transit*, emphasizing the role of the phase-focusing mechanism as a charge-bunching mechanism for the generation of harmonics of the driving voltage signal, which consists of only one tone (the fundamental). Thus, there is no passive intermodulation [13].

Manuscript received November 15, 2019; revised February 4, 2020; accepted March 8, 2020. Date of publication March 24, 2020; date of current version June 10, 2020. This work was supported by the Air Force Office of Scientific Research (AFOSR), Multidisciplinary University Research Initiative (MURI) under Grant FA9550-18-1-0062. The review of this article was arranged by Senior Editor D. A. Shiffler. *(Corresponding author: Patrick Y. Wong.)*

The authors are with the Department of Electrical and Computer Engineering, Michigan State University, East Lansing, MI 48824 USA (e-mail: wongpat3@egr.msu.edu; pz@egr.msu.edu; johnv@egr.msu.edu).

Color versions of one or more of the figures in this article are available online at http://ieeexplore.ieee.org.

Digital Object Identifier 10.1109/TPS.2020.2980482

Section II will present the model and theory of harmonic generation in the multipactor electron cloud. This new theory and model will be numerically validated in Section III with some test cases. Finally, a summary with the main conclusions and possible future work will be discussed in Section IV.

## II. Model

For simplicity and as a proof of principle, we will consider a two-surface planar metal multipactor in one dimension ($x$). The solution (analytical, simulation, and experimental) to this proto-typical problem exists and is well documented e.g., [1], [14], and [15]. This will allow us to better understand the problem and isolate the main mechanisms in play, in particular the intrinsic phase-focusing mechanism of multipactor and its role as a charge buncher. The set-up that will be used and referred to in this article is shown in Fig. 1.

In this figure, we have a gap of length $D$ between two metal plates of cross-sectional area $A$ to which a sinusoidal voltage waveform $V(t) = V_{\mathrm{RF}} \sin(\omega t + \alpha)$, where $V_{\mathrm{RF}}$ is the amplitude, $\omega$ is the (angular) frequency, and $\alpha$ is the initial phase of the signal relative to the electrons, is applied. Electrons (charge $-e$ and mass $m_e$) in the form of infinitesimally thin ($\tau \to 0$) sheets of surface charge density $\sigma_1$ are emitted from a surface with trajectories given by $x_1(t)$.

The equation of motion for an electron in the infinitesimally thin "beam" sheet reads (refer to Appendix A for derivation)

$$\frac{d^2x_1(t)}{dt^2} - \Omega_1^2 x_1(t) = \frac{eV(t)}{m_e D} - \frac{a_1}{2} \tag{1}$$

subject to the initial conditions

$$\begin{cases} x_1(t_0) = x_{10} = \{0, D\} \\ v_1(t_0) \equiv \left.\dfrac{dx_1}{dt}\right|_{t=t_0} = v_{10} \end{cases} \tag{2}$$

where $\Omega_1^2 \equiv a_1/D$, and $a_1 \equiv (e\sigma_1)/(m_e\epsilon_0)$ is the acceleration due to the image charges ($\varepsilon_0$ is the permittivity of free space).

Note that the problem is formulated in the Lagrangian variables ($t$, $t_0$), representing the arrival and departure times of an electron sheet, respectively. At present, we assume that space-charge effects are negligible and the calculation is completely ballistic. Space-charge effects may become significant in certain regimes, completely overpowering the phase-focusing mechanism, but this along with Kishek's cannibalism mechanism [9] will be considered in future works.

The *exact* solution to (1), subject to (2), reads

$$\begin{aligned} x_1(t, t_0) &= \left(x_{10} - \frac{D}{2}\right)\cosh\Omega_1(t - t_0) + \frac{v_{10}}{\Omega_1}\sinh\Omega_1(t - t_0) \\ &\quad + \frac{D}{2} - X_1(\sin(\omega t + \alpha) - \sin(\alpha + \omega t_0)\cosh\Omega_1(t - t_0) - \frac{\omega}{\Omega_1} \\ &\quad \times \cos(\alpha + \omega t_0)\sinh\Omega_1(t - t_0)). \end{aligned} \tag{3}$$

Here, $X_1[m] \equiv [(eV_{\mathrm{RF}})/(m_e D)]1/(\omega^2 + \Omega_1^2)$ is the coefficient in front of the oscillatory part (due to the signal) of the trajectory and characterizes a given electron's tendency to bunch. This new "bunching parameter" may be nondimensionalized as follows:

$$X \equiv X_1[m]\frac{\omega}{v_0} = \frac{eV_{\mathrm{RF}}}{m_e D v_0}\frac{\omega}{\omega^2 + \Omega_1^2} \tag{4}$$

relating to the typical forms used in the klystron and TWT literature [6], [8]. In this form, (4), $X$ applies to each emitted electron individually with the emission velocity $v_0$. The greater the amplitude of the RF electric field ($|V_{\mathrm{RF}}/D|$), the more likely a given electron will tend to bunch. This is also true for low velocity electrons, for a fixed RF electric field.

Of course, this solution is only valid while the electrons are in the gap. Upon impact with the surface of an electrode, the current electron sheet is removed and replaced with one with surface charge density $\sigma_{1,i+1} = \delta \cdot \sigma_{1,i}$, where the secondary electron yield (SEY) $\delta$ is governed by Vaughan's model [16; see also Appendix B] and $i$ is the transit number (beginning with $i = 1$).

Note that we treat multipactor as a classical resonance phenomenon. We do not consider "ping-pong modes" [17], [18] so that the multipactor electrons that cannot cross the gap and return to the birthing electrode are removed and do not contribute to the current. This is a valid assumption in this 1-D set-up where the current is measured at some location downstream and we are dealing with electron sheets (so the current contribution from returning electrons in one transit are negated).

Equation (3) gives the orbits of the multipactor electrons in the gap, subject to a sinusoidal voltage and image charges (ignoring space charge). Because of the phase-focusing mechanism (to the fixed phase) inherent to multipactor discharges, the multiple electron sheets comprising the "beam" or electron cloud will tend to converge to the fixed phase if they are within the basin of attraction of that fixed phase. Otherwise, the electron sheets are emitted with an unfavorable phase and hence are forced back into the birthing electrode. For the electrons that do survive, they will multipact and physically bunch while their phases converge toward the fixed phase. That is, the intrinsic phase-focusing mechanism of a multipactor acts as a natural charge-bunching mechanism. In this case, charge conservation must hold at every instance in the gap (except when the electrons hit the electrodes); thus, *for each transit*,

$$I_0 dt_0 = I dt \Rightarrow I(t) = I_0(t_0)\frac{dt_0}{dt} \equiv \sum_{n=-\infty}^{\infty} \tilde{I}_n e^{jn\omega t}, \tag{5}$$

$$\begin{aligned} \tilde{I}_n &\equiv \frac{\omega}{2\pi}\int_0^{2\pi/\omega} I(t)e^{-jn\omega t}dt \\ &= \frac{\omega}{2\pi}\int_{t_0(0)}^{t_0(2\pi/\omega)} I_0(t_0)e^{-jn\omega t(t_0)}dt_0 \end{aligned} \tag{6}$$

where we have written the current at some downstream location $I(t)$ as a Fourier series with the Fourier coefficients given by (6). In the last equality of (6), the standard formula for the Fourier coefficients (over the period under consideration) has been rewritten using the change of variables introduced by charge conservation in (5), so that the integration is over the departure times. We take the initial current at the upstream position to be the current from a birthing electrode: $I_0(t_0) \equiv (\sigma_1(t_0)A)/\Delta t_0$ [19].

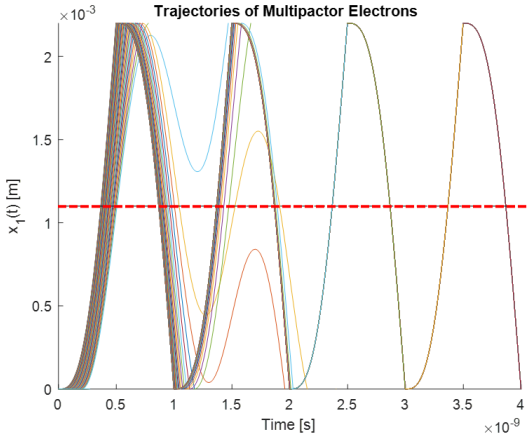


Fig. 2. Trajectories of multipactor electrons for the test case (a) with mono-energetic emission (0 eV) showing orbital crowding from phase focusing as time progresses. The red dotted line indicates where the current downstream is calculated.

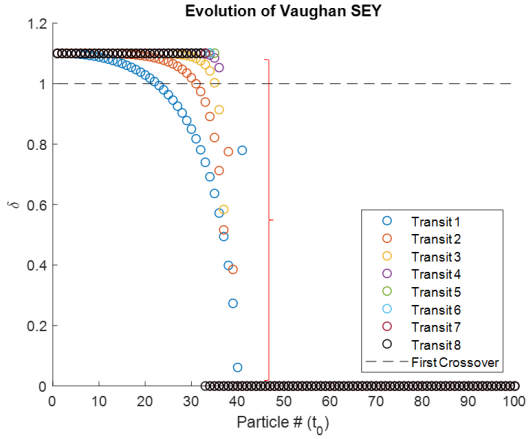


Fig. 3. Evolution of the SEY according to Vaughan's model for all the sheets launched, at the end of each transit, for the test case (a). This further shows phase focusing as the nonresonant particles are weeded out as the multipactor progresses.

With this, we can calculate the multipactor electron orbits using (3) and the "beam" current at some location downstream from the birthing electrode using (5) and (6), *for each transit*. At the boundary between transits, the electron sheets are updated according to Vaughan's model and an emission scheme (discussed more in Section III). Delay times in emission are not considered here, though their effects may be ascertained using the theory provided in [20].

## III. Test Cases

To assess the viability of the theory outlined in the previous section, we consider several test cases. To begin, electrons are born from the bottom electrode at $x = 0$. For this initial birthing process and subsequent secondary electron emission from impacts of electrons with the electrodes, different emission schemes are used in the test cases. In the test case (a), it is assumed that electrons are born with mono-energetic emission energy, taken here to be $v_0 = 0$ eV. In the test case (b), this assumption is relaxed and random emission energies of electrons from electrodes following a distribution are allowed. This leads into the polyphase regime with hybrid modes [21]–[23].

In both test cases, the gap distance $D = 0.22$ cm, and the surface area of each electrode is $A = 0.22$ cm$^2$. The maximum SEY from each electrode is $\delta_{\max} = 1.2$, occurring at an energy of $E_{\max} = 400$ eV. A $V_{\mathrm{RF}} = 350$ V RF voltage with a frequency of 1 GHz is applied to this set-up.

Macroparticles (the electron sheets of surface charge density $\sigma_1 = 8.76 \times 10^{-13}$ C/cm$^2$) are launched at a range of departure times. Only those particles that can reach the inspection point, set here to be $d = D/2$, and the other electrode have their properties plotted in Figs. 2–4.

### A. Mono-Energetic Secondary Electron Emission Test Case

Figures 2–4 present the main results of the above-described test case with mono-energetic secondary electron emission from the electrodes. Fig. 2 shows the trajectories of the multipactor electrons that can cross the gap and hence the current inspection point midway. Fig. 3 shows the SEY according to

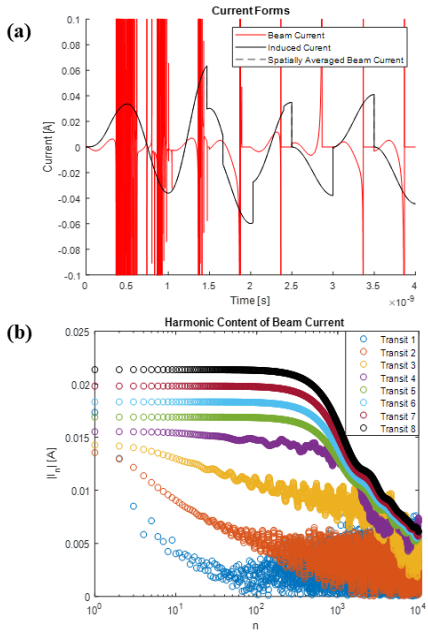


Fig. 4. (a) Plot of the current forms from the beam current as calculated from the midplane (red) and the induced current on an electrode (black) for the test case (a). (b) Plot of the harmonic content in the beam current as measured from the midplane for the test case (a). As the multipactor progresses, phase focusing and subsequent current crowding become more prominent. As a result, more and more harmonics are generated.

Vaughan's model at the end of each transit as a function of the macroparticle number (numbered 1–100 for the examples shown here), corresponding to the different (evenly spaced) departure times from an electrode. Finally, Fig. 4(a) plots the "beam" current $I(t)$ as calculated at the inspection point midplane from (5) (red) as well as the induced current in the external circuit (black), which is discussed in the following; Fig. 4(b) plots the harmonic content of this "beam" current (here, $I_n = 2\tilde{I}_n, n > 0$ because $\tilde{I_{|n|}} = \tilde{I_{-|n|}}$).

### B. Secondary Electron Emission With Random Emission Energies Test Case

A more realistic case is having secondary electron emission with random emission energies according to a distribution.

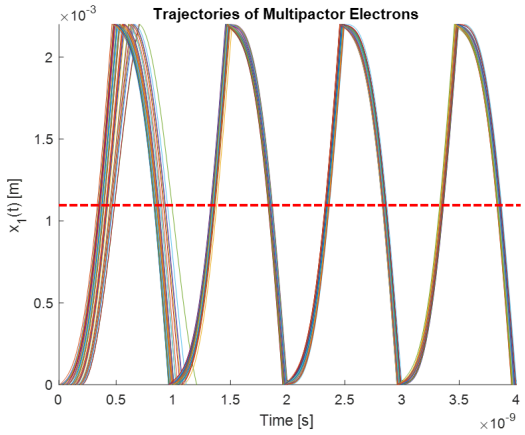


Fig. 5. Trajectories of multipactor electrons for the test case (b) with random emission in energy also showing orbital crowding from phase focusing as time progresses. The red dotted line indicates where the current downstream is calculated.

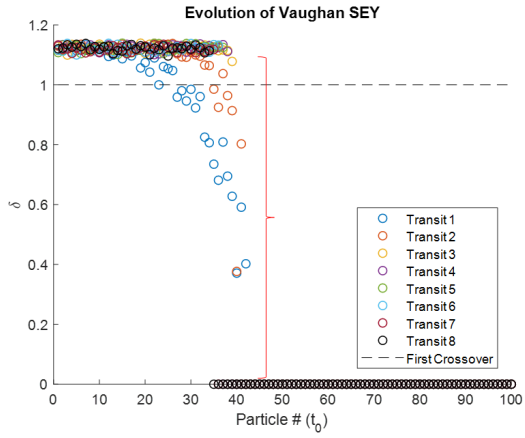


Fig. 6. Evolution of SEY according to Vaughan's model for all the sheets launched, at the end of each transit, for the test case (b). This also further shows phase focusing as the nonresonant particles are weeded out as the multipactor progresses.

All the secondary electrons are assumed to be emitted vertically from the surface ($\theta = 0$). The (average) number of secondary electrons created from each impact with an electrode is still governed by the Vaughan model; however, the emission energies of these secondary electrons $E_0$ are randomly assigned according to the equation [24] $f(E_0) = (E_0/E_{0,m}^2)e^{-(E_0/E_{0,m})}$, where $E_{0,m} = 0.005\ E_{\max}(\theta = 0)$ and $E_{\max}$ is the maximum energy corresponding to $\delta_{\max}$ at normal incidence ($\theta = 0$). Similar to the test case (a), Figs. 5–8 present the main results.

In Fig. 8, the defined "bunching parameter" from (4) is plotted as a function of the macroparticle number, corresponding to different departure times from an electrode. This bunching parameter for the test case (a) tends to infinity because the emitting electrons from an electrode are assumed to be monoenergetic with zero energy, indicating that these multipactor electrons will indefinitely bunch.

### C. Discussion of Results of Test Cases

As can be seen in both test cases, as the multipactor system evolves in time, the formation of tight electron bunches becomes apparent as the phase-focusing mechanism becomes

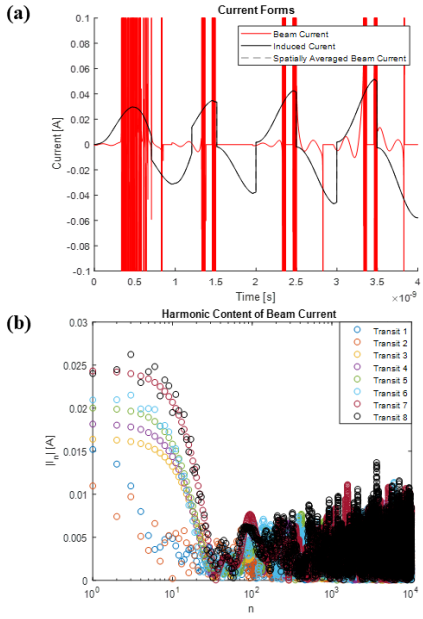


Fig. 7. (a) Plot of the current forms from the beam current as calculated from the mid-plane (red) and the induced current on an electrode (black) for test case (b). (b) Plot of the harmonic content in the beam current as measured from the mid-plane for test case (b). As multipactor progresses, phase focusing and subsequent current crowding (and charge overtaking) become more prominent. As a result, more and more harmonics are generated.

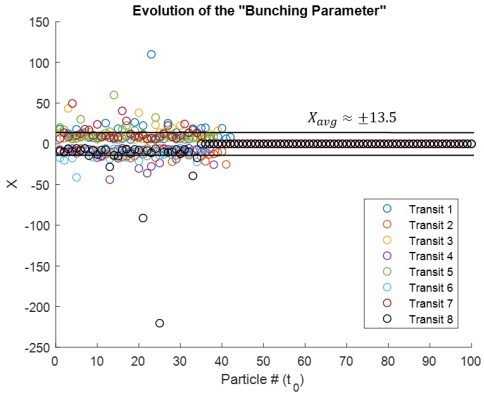


Fig. 8. Plot of the "bunching parameter" [cf. (4)] for the test case (b) as a function of the particle number. Most particles (centered on average) will tend to bunch, whereas some will overtake.

prominent. This may be seen in the plots of the multipactor electron trajectories (Figs. 2 and 5) where there is still a substantial number of electrons centered around the fixed phase after several transits, even with random emission energies as in the test case (b), demonstrating orbital crowding in both systems. The plots showing the evolution of the SEY as a function of the particle number launched, which is proportional to the departure phase (Figs. 3 and 6), also show this trend: the trailing electrons are essentially weeded out until a tight bunch of electrons around the fixed phase remains. Because of this charge compression, harmonics (of the input signal) in the electron clouds are developed, as can be seen in Figs. 4 and 7, where we inspect the beam current forms at the midplane $d = D/2$. As can be seen in Figs. 4(b) and 7(b), which are plotted with a logarithmic axis for the abscissa to emphasize the lower harmonics, a large range of harmonics of the input frequency are generated in the electron cloud current.

This range increases with each consecutive transit. Past this range though, the higher harmonics constitute noise or a weaker waveform.

The delta-function-like spikes in the current from each electron sheet passing through the inspection plane become closer and closer as time advances (ideally becoming one delta-function-like spike). In the test case (a), it was observed that orbital and/or current crowding resulting from the phase focusing of the electrons in the electron cloud led to harmonic generation. In the test case (b) though, when random emission energies are included for the secondary electrons, charge overtaking in addition to orbital and/or current crowding occurs. This accounts for the multiple delta-function-like spikes in the current. One may see this in Fig. 8, where for some transits, there is a subset of slow particles that have $|X| \gg |X_{\text{avg}}| \approx 13.5$ so that faster particles overtake this subset.

It should be noted that the current induced in the external circuit calculated via the Shockley–Ramo Theorem [25], [26] [shown in black in Figs. 4(a) and 7(a)] is the spatial integration of this "beam" current [shown in red in Figs. 4(a) and 7(a)]. That is, $I_{\text{Shockley–Ramo}} = I_{\text{induced}} = 1/D \int_0^D I(t)dx$ (this is the current used in Sorolla *et al.*'s article [12]); this spatially averaged beam current is plotted with black dashed lines in Figs. 4(a) and 7(a), where it can be seen that there is good agreement with the traditional definition of the induced current. For identifiable (infinitesimally thin) charge sheets of surface charge density $\sigma_j$, velocity $v_j$, and (constant) surface area $A$ that comprise the "beam", $I(t) = \sum_j \sigma_j \delta(x - x_j(t)) v_j(t) A$, so that upon evaluation, $I_{\text{Shockley–Ramo}} = I_{\text{induced}} = A/D \sum_j \sigma_j v_j$, which is the familiar expression for the induced current in the circuit via the Shockley–Ramo theorem. This implies that, in addition to the fundamental, harmonics are present in the signal if this were a transmission line system or if the beam loading of the cavity is considered.

A final note concerns the validity and usefulness of such a set-up as presented here. From a single-tone RF voltage at the fundamental frequency applied to a multipactor set-up, harmonics of the fundamental are generated in the current of the electron cloud. There exist a wide range of usable (coherent) harmonic currents, more so for the case with monoenergetic emission. These currents may contribute to the radiation originating from the multipactor electrons or may be used as a signal generator. Even though the analytical treatment and model here were limited to one spatial dimension, it is expected to apply to 3-D settings as long as phase-locking to the applied signal and phase focusing occurs.

## IV. Conclusion and Future Work

In conclusion, we have shown that harmonics of the driving voltage signal may be generated in the current of the electron clouds of a multipactor discharge, taking advantage of the inherent phase-focusing mechanism as a natural charge-bunching mechanism. Even relaxing the assumption of monoenergetic secondary electron emission, it was found that a significant population of electrons in the cloud or "beam" still survived and contributed to harmonic generation via the process of orbital or current crowding and/or charge overtaking. It was seen in the results that a wide range of coherent, usable harmonics were generated for both cases. A "bunching parameter" similar to that found in klystron and TWT theories was derived to characterize a given set-up's tendency to bunch.

This article may give an alternative explanation of the radiation at the fundamental frequency $\omega$ and its harmonics observed in multipactor discharges. As opposed to a global model (i.e., with *a priori* knowledge of the output) as presented in [11] and [12], this model provides a local (per transit) explanation, identifying the phase-focusing effect as the culprit for charge bunching and harmonic generation. This may be important for the detection of multipactor onset, especially for the third harmonic [27]. Conversely, a multipactor may also be used as a potential radiation source, similar to a vircator.

An important and interesting future work involves self-consistently including space-charge effects (i.e., mutual space-charge repulsion between the macroparticles). Doing so is not a trivial exercise but will better capture the physics, in particular, the interaction between the intrinsic phase-focusing mechanism of multipactor (discussed here), space-charge repulsion, and Kishek's cannibalism mechanism [9]. The cannibalism mechanism is another phase-focusing mechanism that manifests when there are multiple macroparticles and space charge present. Exploring the parameter regime of the interplay between these different forces and its effects on harmonic generation will be interesting. Relaxing the assumption of the normal incidence of electron impact with and emission from the electrode surfaces will also be interesting. The beginning of such a formulation is presented in Appendix B. In summary, it was found that even with the inclusion of oblique incidences for emitting/impacting multipactor electrons with the electrode surfaces (a 2-D calculation), phase focusing still occurs, resulting in charge bunching (orbital crowding and charge overtaking) and harmonic generation.

## Appendix A: Derivation of the Equation of Motion for an Infinitesimally Thin Electron Sheet

In this appendix, for completeness, the equation of motion for an electron (mass $m_e$ and charge $-e$) of an infinitesimally thin electron sheet (representing a slice of the "beam") will be derived. See also [14], [15], and [28], and Appendixes A and B of [29].

Suppose at an instant of time $t > 0$ when a charged sheet is crossing the gap $0 < x < D$, the instantaneous position of the sheet is $x_1(t)$ and this thin flat sheet has charge $q$. The presence of this charge in the gap induces charge on both the top and bottom metal plates: $Q - q(x_1(t)/D)$ and $-Q - q(1 - x_1(t)/D)$, respectively, where $\pm Q$ is the charge that is already present on the plates due to the external applied voltage to the plates. The electric fields above and below the charged sheet are then

$$\overrightarrow{E_{\text{up}}} = -\frac{Q - q\left(\frac{x_1(t)}{D}\right)}{\epsilon_0 A}\hat{x} \tag{A1}$$

$$\overrightarrow{E_{\text{down}}} = -\frac{Q + q\left(\frac{D - x_1(t)}{D}\right)}{\epsilon_0 A}\hat{x} \tag{A2}$$

where $\varepsilon_0$ is the permittivity of free space and $A$ is the area of the plates. The force on an electron in the charged sheet (a discontinuity between the top and bottom regions) is then [28]

$$\vec{F} = -e\left[\frac{1}{2}(\vec{E_{\text{up}}} + \vec{E_{\text{down}}})\right] = \left[\frac{eQ}{\epsilon_0 A} + \frac{eq}{2\epsilon_0 A}\left(1 - 2\frac{x_1}{D}\right)\right]\hat{x}. \tag{A3}$$

The voltage across the gap (from the bottom plate to the top plate) is

$$V(t) \equiv -\int \vec{E} \cdot \vec{dx} = -\int_0^{x_1} E_{\text{down}} dx - \int_{x_1}^{D} E_{\text{up}} dx = \frac{QD}{\epsilon_0 A}. \tag{A4}$$

However, $V$ is prescribed; thus, we can eliminate $Q$ from (A3) and (A4) to give

$$\vec{F} \equiv m_e \frac{d^2 x_1(t)}{dt^2}\hat{x} = \left[e\frac{V(t)}{D} - \frac{eq}{\epsilon_0 A}\left(\frac{x_1}{D} - \frac{1}{2}\right)\right]\hat{x} \tag{A5}$$

which is (1) of the main text upon using the appropriate definitions of the parameters and $q = -\sigma_1 A$.

## Appendix B: Material Properties of the Electrodes and a 2-D Model

In this appendix, we address in more detail the material used for the electrodes and the case of oblique incidence (as opposed to normal incidence, $\theta = 0$) of electron impact and emission with respect to the normal of the surface of the electrodes.

We use a material that has $\delta_{\max} = 1.2$ corresponding to an electron impact energy of $E_{\max} = 400$ eV at the normal incidence (i.e., $\theta = 0$). This roughly corresponds to iron (Fe) with a smoothness factor of $k_s = 1$ [30]. To make the calculation analytically tractable, we ideally assume these values for the electrodes remain the same. The Vaughan model [16] has been used to model SEY

$$\delta(E_i, \theta) = \delta_{\max}(\theta)(we^{1-w})^k \tag{B1}$$

where

$$w \equiv \frac{E_i - E_{\text{threshold}}}{E_{\max}(\theta) - E_{\text{threshold}}} \tag{B2}$$

and

$$k = \begin{cases} 0.62, & w < 1 \\ 0.25, & 1 < w \leq 3.6 \end{cases} \tag{B3}$$

with $E_{\text{threshold}} = 12.5$ eV. For high electron impact energy $E_i$ corresponding to $w > 3.6$,

$$\delta(E_i, \theta) = \delta_{\max}(\theta)\frac{1.113}{w^{0.35}}. \tag{B4}$$

To correct for oblique incidences of electron impact (i.e., $\theta \neq 0$ as measured from the normal) and to account for the smoothness of the material,

$$\delta_{\max}(\theta) = \delta_{\max}\left(1 + k_s\frac{\theta^2}{2\pi}\right) \tag{B5}$$

$$E_{\max}(\theta) = E_{\max}\left(1 + k_s\frac{\theta^2}{\pi}\right) \tag{B6}$$

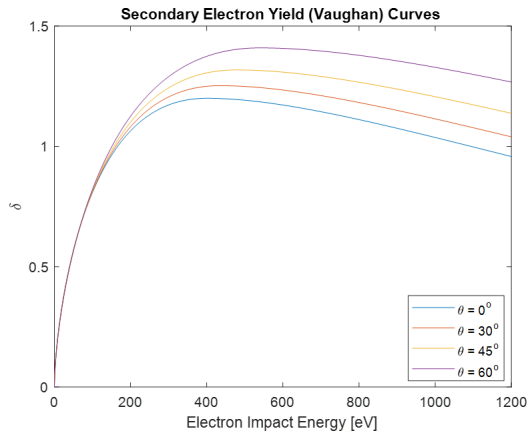


Fig. 9. Some sample SEY curves ($\delta$ as a function of the electron impact energy) for different angles according to the standard Vaughan model.

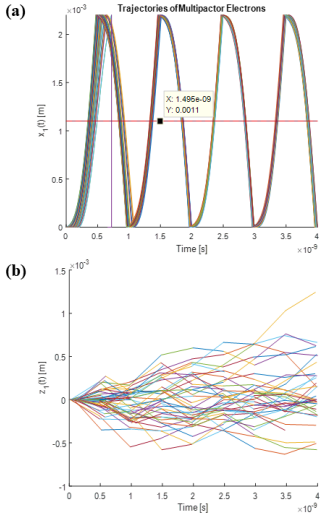


Fig. 10. (a) Trajectories of multipactor electrons in the $x$-direction for the test case (b) with random emission in energy and angle also showing orbital crowding from phase focusing as time progresses. The red dotted line indicates where the current downstream is calculated. (b) Trajectories of multipactor electrons in the $z$-direction.

which reduce to $\delta_{\max}$ and $E_{\max}$ when $\theta = 0$ (normal impact).

Some sample SEY curves ($\delta$ as a function of the electron impact energy $E_i$) for different angles $\theta$ are plotted in Fig. 9 using the material described above.

Accounting for oblique incidences of electron impact with and emission from the surfaces of the electrodes necessarily makes the calculation 2-D (at least). The present theory is a 1-D theory (in $x$); however, oblique incidences of impacting and emitting electrons may still be accounted for, if needed, as demonstrated below.

Assuming that there are no magnetic fields (only electric fields due to the voltage source and image charges in the $x$-direction), the equation of motion for an electron in the infinitesimally thin electron sheet in the $z$-direction reads

$$\frac{d^2 z_1}{dt^2} = 0 \tag{B7}$$

yielding

$$z_1(t, t_0) = (v_0 \sin\theta)(t - t_0) + z_{10} \tag{B8}$$

for the orbit in the $z$-direction. Now, the initial velocity of an emitted electron from an electrode (and also that

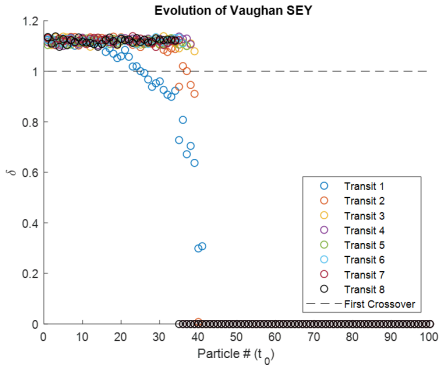


Fig. 11. Evolution of SEY according to Vaughan's model for all the sheets launched, at the end of each transit, for the test case (b) with added random emission angles. This also shows phase focusing as the nonresonant particles are weeded out as the multipactor progresses.

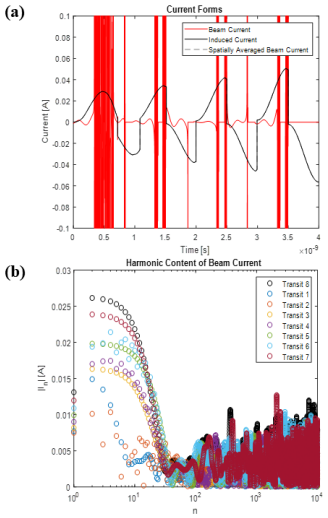


Fig. 12. (a) Plot of the current forms from the beam current as calculated from the midplane (red) and the induced current on an electrode (black) for the test case (b) with added random emission angles. (b) Plot of the harmonic content in the beam current as measured from the midplane for the test case (b) with added random emission angles. As the multipactor progresses, phase focusing and subsequent current crowding (and charge overtaking) become more prominent. As a result, more and more harmonics are generated. Note the last two transits 7 and 8.

of the electron impacting a surface) has two components: $\overrightarrow{v_0} = (v_0 \cos\theta)\hat{x} + (v_0 \sin\theta)\hat{z}$, where the initial speed $v_0$ is related to the emission energy $E_0 = 1/2 m_e v_0^2$ and $\theta$ is the angle of emission with respect to the normal of the electrode surfaces. The initial $z$-position of the electron is $z_{10}$, which will change as time evolves and the multipacting electrons bounce back and forth between the two electrodes.

Ultimately, allowing this extra degree of motion in the $z$-direction makes the multipacting electrons "drift" (translate) along the $z$-axis and reduces the velocity (and hence energy) of the electrons in the $x$-direction. This perturbs the arrival time of the multipacting electrons and also the average SEY of the multipacting system, leading to a reduction in the amplitude of the harmonic current (phase focusing still occurs and will bunch the electrons causing harmonic generation as outlined in the main text).

As an example, consider the test case (b) from the main text. In addition to the emission energy of the secondary electrons being randomly assigned according to the distribution

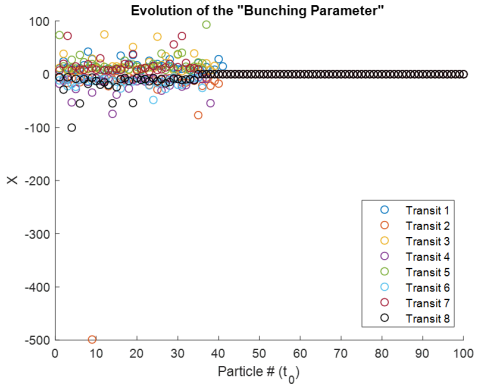


Fig. 13. Plot of the "bunching parameter" [cf. (4) of the main text] for the test case (b) with random emission angles as a function of the particle number. Most particles (centered on average) will tend to bunch, whereas some will overtake.

$f(E_0)$, the emission angle of the secondary electrons are also randomly assigned according to: $g(\theta) = 1/2 \cos\theta$. The results are shown in Figs. 10–13.

Although there are some differences between the test case (b) with normal incidences for electron impact and emission with the surfaces (main text) and the test case (b) with random emission angles (in this appendix), the results are qualitatively similar, as evidenced by comparing Figs. 5–8 from the main text to Figs. 10–13 in this appendix. This shows that even relaxing the assumption of normal incidence of electron impact with the surfaces of the electrodes (a 1-D calculation) to include random emission angles according to a distribution (a 2-D calculation), phase focusing of the multipactor electrons to the fixed phase still occurs. This phase focusing in turn leads to charge bunching (orbital and/or current crowding) or charge overtaking, giving rise to the harmonic generation of the fundamental frequency of the input signal.

## REFERENCES

[1] J. R. M. Vaughan, "Multipactor," *IEEE Trans. Electron Devices*, vol. 35, no. 7, pp. 1172–1180, Jul. 1988, doi: 10.1109/16.3387.

[2] R. A. Kishek, Y. Y. Lau, L. K. Ang, A. Valfells, and R. M. Gilgenbach, "Multipactor discharge on metals and dielectrics: Historical review and recent theories," *Phys. Plasmas*, vol. 5, no. 5, pp. 2120–2126, May 1998, doi: 10.1063/1.872883.

[3] *Special Sessions on Multipactor, I and II*, ICOPS, Denver, CO, USA, Jun. 2018.

[4] P. Y. Wong, Y. Y. Lau, P. Zhang, N. Jordan, R. M. Gilgenbach, and J. Verboncoeur, "The effects of multipactor on the quality of a complex signal propagating in a transmission line," *Phys. Plasmas*, vol. 26, no. 11, Nov. 2019, Art. no. 112114, doi: 10.1063/1.5125408.

[5] F. M. Mako and W. Peter, "A high-current micro-pulse electron gun," in *Proc. IEEE Part. Accel. Conf.*, May 1993, pp. 2702–2704, doi: 10.1109/PAC.1993.309434.

[6] J. W. Gewartowski and H. A. Watson, *Principles of Electron Tubes: Including Grid-Controlled Tubes, Microwave Tubes, and Gas Tubes*. New York, NY, USA: Van Nostrand, 1965.

[7] C. B. Wilsen, Y. Y. Lau, D. P. Chernin, and R. M. Gilgenbach, "A note on current modulation from nonlinear electron orbits," *IEEE Trans. Plasma Sci.*, vol. 30, no. 3, pp. 1176–1178, Jun. 2002, doi: 10.1109/TPS.2002.801571.

[8] C. F. Dong *et al.*, "Harmonic content in the beam current in a traveling-wave tube," *IEEE Trans. Electron Devices*, vol. 62, no. 12, pp. 4285–4292, Dec. 2015, doi: 10.1109/TED.2015.2490584.

[9] R. A. Kishek and Y. Y. Lau, "A novel phase focusing mechanism in multipactor discharge," *Phys. Plasmas*, vol. 3, no. 5, pp. 1481–1483, May 1996, doi: 10.1063/1.872027.

[10] V. E. Semenov, E. I. Rakova, N. A. Zharova, J. Rasch, D. Anderson, and J. Puech, "Simple model of the RF noise generated by multipacting electrons," *J. Phys. D: Appl. Phys.*, vol. 47, no. 5, Feb. 2014, Art. no. 055206, doi: 10.1088/0022-3727/47/5/055206.
[11] B. Gimeno *et al.*, "Multipactor radiation analysis within a waveguide region based on a frequency-domain representation of the dynamics of charged particles," *Phys. Rev. E, Stat. Phys. Plasmas Fluids Relat. Interdiscip. Top.*, vol. 79, no. 4, Apr. 2009, Art. no. 046604, doi: 10.1103/PhysRevE.79.046604.
[12] E. Sorolla *et al.*, "An analytical model to evaluate the radiated power spectrum of a multipactor discharge in a parallel-plate region," *IEEE Trans. Electron Devices*, vol. 55, no. 8, pp. 2252–2258, Aug. 2008, doi: 10.1109/TED.2008.926271.
[13] L. Zhang *et al.*, "Numerical simulation and analysis of passive intermodulation caused by multipaction," *Phys. Plasmas*, vol. 25, no. 8, Aug. 2018, Art. no. 082301.
[14] R. Kishek and Y. Y. Lau, "Interaction of multipactor discharge and RF circuit," *Phys. Rev. Lett.*, vol. 75, no. 6, pp. 1218–1221, Aug. 1995.
[15] E. Sorolla and M. Mattes, "Multipactor saturation in parallel-plate waveguides," *Phys. Plasmas*, vol. 19, no. 7, Jul. 2012, Art. no. 072304.
[16] J. R. M. Vaughan, "A new formula for secondary emission yield," *IEEE Trans. Electron Devices*, vol. 36, no. 9, pp. 1963–1967, Sep. 1989, doi: 10.1109/16.34278.
[17] R. A. Kishek, "Ping-pong modes: A new form of multipactor," *Phys. Rev. Lett.*, vol. 108, no. 3, Jan. 2012, 035003, doi: 10.1103/PhysRevLett.108.035003.
[18] R. A. Kishek, "Ping-pong modes and higher-periodicity multipactor," *Phys. Plasmas*, vol. 20, no. 5, May 2013, Art. no. 056702.
[19] C. K. Birdsall and W. B. Bridges, *Electron Dynamics of Diode Regions*. New York, NY, USA: Academic, 1966.
[20] S. Riyopoulos, D. Chernin, and D. Dialetis, "Effect of random secondary delay times and emission velocities in electron multipactors," *IEEE Trans. Electron Devices*, vol. 44, no. 3, pp. 489–497, Mar. 1997.
[21] A. Kryazhev *et al.*, "Hybrid resonant modes of two-sided multipactor and transition to the polyphase regime," *Phys. Plasmas*, vol. 9, no. 11, pp. 4736–4743, Nov. 2002, doi: 10.1063/1.1514969.
[22] A. Sazontov *et al.*, "Effect of emission velocity spread of secondary electrons in two-sided multipactor," *Phys. Plasmas*, vol. 12, no. 5, May 2005, Art. no. 053102, doi: 10.1063/1.1881532.
[23] S. Riyopoulos, "Higher-order, asymmetric orbit multipactors," *Phys. Plasmas*, vol. 14, no. 11, Nov. 2007, Art. no. 112101.
[24] A. Iqbal, J. Verboncoeur, and P. Zhang, "Temporal multiparticle Monte Carlo simulation of dual frequency single surface multipactor," *Phys. Plasmas*, vol. 26, no. 2, Feb. 2019, Art. no. 024503, doi: 10.1063/1.5084143.
[25] W. Shockley, "Currents to conductors induced by a moving point charge," *J. Appl. Phys.*, vol. 9, no. 10, pp. 635–636, Oct. 1938.
[26] S. Ramo, "Currents induced by electron motion," *Proc. IRE*, vol. 27, no. 9, pp. 584–585, Sep. 1939, doi: 10.1109/JRPROC.1939.228757.
[27] R. Udiljak *et al.*, "New method for detection of multipaction," *IEEE Trans. Plasma Sci.*, vol. 31, no. 3, pp. 396–404, Jun. 2003, doi: 10.1109/TPS.2003.811646.
[28] D. J. Griffiths, *Introduction to Electrodynamics*. Upper Saddle River, NJ, USA: Prentice-Hall, 1999, pp. 102–103.
[29] R. A. Kishek, "Interaction of multipactor discharge and RF structures," Ph.D. dissertation, Dept. Nucl. Eng. Radiol. Sci., Univ. Michigan, Ann Arbor, MI, USA, 1997.
[30] O. Hachenberg and W. Brauer, "Secondary electron emission from solids," *Adv. Electron. Electron Phys.*, vol. 11, pp. 413–499, Jan. 1959.

**Patrick Y. Wong** (Member, IEEE) received the B.S.E., M.S.E., and Ph.D. degrees from the University of Michigan, Ann Arbor, MI, USA, in 2014, 2015, and 2018, respectively.

He is currently a Post-Doctoral Researcher with the Department of Electrical and Computer Engineering, Michigan State University, East Lansing, MI, USA. His research interests include theoretical and computational modeling of beam-circuit interactions in high-power microwave devices including traveling-wave tubes, magnetrons, and multipactor.

**Peng Zhang** (Senior Member, IEEE) received the B.Eng. and M.Eng. degrees in electrical and electronic engineering from Nanyang Technological University, Singapore, in 2006 and 2008, respectively, and the Ph.D. degree in nuclear engineering and radiological sciences from the University of Michigan (UM), Ann Arbor, MI, USA, in 2012.

He was an Assistant Research Scientist with the Department of Nuclear Engineering and Radiological Sciences, UM. He is currently Assistant Professor with the Department of Electrical and Computer Engineering, Michigan State University (MSU), East Lansing, MI, USA. He has authored refereed journal publications on electrical contacts, thin films, classical, ballistic, and quantum diodes, space-charge-limited current flows, beam-circuit interaction, multipactor and breakdown, microwave absorption on rough surfaces, slow wave structures, $z$-pinches, laser-plasma interaction, and more recently on vacuum nanodevices, quantum tunneling plasmonic junctions, ultrafast photoemission, and novel miniaturized electromagnetic radiation sources. His current research interests include theoretical and computational physics in nanoelectronics, plasmas, and accelerator technology.

Dr. Zhang is currently serving as an Editorial Board Member for Scientific Reports, a Journal by Nature and Plasma Research Express, a Journal by the Institute of Physics. He was a recipient of the AFOSR Young Investigator Program Award, the UM Richard and Eleanor Towner Prize for Outstanding Ph.D. Research, the UM Rackham Presidential Fellowship Award, and the IEEE Nuclear and Plasma Sciences Graduate Scholarship Award.

**John P. Verboncoeur** (Fellow, IEEE) received the B.S. degree in engineering science from the University of Florida, Gainesville, FL, USA, in 1986, and the M.S. and Ph.D. degrees in nuclear engineering from the University of California at Berkeley (UCB), Berkeley, CA, USA.

He was a Post-Doctoral Researcher with the Lawrence Livermore National Laboratory, Livermore, CA, USA, and with the Department of Electrical Engineering and Computer Science (EECS), UCB. He was an Associate Research Engineer with EECS, UCB, where he was a Nuclear Engineering Faculty in 2001 and a Full Professor in 2008. From 2001 to 2010, he served as the Chair for the Computational Engineering Science Program, UCB. In 2011, he joined Michigan State University (MSU), East Lansing, MI, USA, as a Professor of electrical and computer engineering, where he was a Professor of computational mathematics, science, and engineering in 2015. He has authored or coauthored in MSU (formerly Berkeley) suite of particle-in-cell Monte Carlo codes, including XPDP1 and X-windows Object Oriented Particle-In-Cell (XOOPIC), used by over 1000 researchers worldwide with over 350 journal publications in the last decade, 350 journal articles and conference papers, with over 3500 citations, and has taught 13 international workshops and minicourses on plasma simulation. His current research interests include theoretical and computational plasma physics, with a broad range of applications spanning low-temperature plasmas for lighting, thrusters, and materials processing to hot plasmas for fusion, from ultracold plasmas to particle accelerators, from beams to pulsed power, from intense kinetic nonequilibrium plasmas to high-power microwaves.

Dr. Verboncoeur was a Past-President of the IEEE Nuclear and Plasma Science Society and an IEEE Director-Elect. He was a recipient of the Department of Energy (DOE) Magnetic Fusion Energy Technology Fellowship. He is currently an Associate Editor of the Physics of Plasmas. He has served as a Guest Editor and/or a frequent reviewer for the IEEE TRANSACTIONS ON PLASMA SCIENCE, the IEEE TRANSACTIONS ON ELECTRON DEVICES, as well as a number of other plasma and computational journals.